Chapter 12

Vortices and Singularities in Electric Dipole Radiation near an Interface

Xin Li, Henk F. Arnoldus and Zhangjin Xu

Additional information is available at the end of the chapter

http://dx.doi.org/10.5772/66459

Abstract

An oscillating electric dipole in free space emits its energy along straight lines. We have considered the effect of a nearby interface with a material medium. Interference between the directly emitted radiation and the reflected radiation leads to intricate flow line patterns. When the interface is a plane mirror, numerous interference vortices appear, and when the distance between the dipole and the mirror is not too small, these vortices lie on four strings. At the center of each vortex is a singularity, and these singularities are due to the fact that the magnetic field vanishes at these locations. When the interface is a boundary between dielectric media, reflection leads again to interference. The pattern for the transmitted radiation depends on whether the medium is thicker or thinner than the material in which the dipole is embedded. For thicker dielectrics, the field lines bend toward the normal, reminiscent of, but not the same as, the behavior of optical rays. For thinner media, oscillation of energy across the interface appears, and above a crossing point, there is a tiny vortex. We have also considered the case of a dipole in between two parallel mirrors.

Keywords: vortex, singularity, Poynting vector, dipole radiation, interface, mirror

1. Introduction

The common conception about the propagation of light is that the radiation travels along straight lines. Such a picture certainly seems to hold for a laser beam and for sunlight. The success of ray diagrams for the construction of images by lenses and mirrors also supports this picture. Reflection by and transmission through an interface is another example of a process that can be described by a ray picture of light. However, light is electromagnetic radiation, and ultimately any optical phenomenon must be accounted for by a solution of Maxwell's equations

for the electric and magnetic fields. In the geometrical optics limit of light propagation [1], spatial variations on the scale of a wavelength or less are neglected, and optical rays are defined as the orthogonal trajectories of the wave fronts of a propagating wave. From a different point of view, we can define the direction of light propagation as the direction of the energy flow in the radiation field. This direction is determined by the electromagnetic Poynting vector [2]. It can be shown that in the geometrical optics limit for propagation in vacuum the field lines of the Poynting vector are straight lines and are identical to the optical rays, defined with the help of the propagation of wave fronts.

The concept of optical rays breaks down when spatial variations on the scale of a wavelength or less are of concern, or when coherence in the radiation leads to macroscopic constructive and destructive interference (as for a diffraction grating). We shall consider a small particle, like an atom, molecule, or nano-particle, irradiated by a monochromatic laser beam, oscillating with angular frequency ω. We shall assume that the beam is linearly polarized. The electric field of the laser beam induces an electric dipole moment in the particle, and this dipole moment oscillates with angular frequency ω along the same direction as the electric field of the immersing beam. The oscillating dipole moment emits electromagnetic radiation (expressions for the electric and magnetic fields are given below), and the Poynting vector is easily calculated. It appears that the field lines of the Poynting vector are straight lines, coming out of the dipole and running radially outward to infinity. This is illustrated in **Figure 1**.

The energy flow lines for a free (linear) dipole are straight at all distances. Any deviation from this radially outgoing pattern is due to the environment of the particle. For instance, when the particle is embedded in an absorbing medium, the imaginary part of the permittivity is responsible for a bending of the field lines in the near field toward the dipole axis [3]. Here we shall consider the case where the particle is located near an interface. Some of the emitted radiation by the dipole will be incident on the interface, and here reflection and transmission takes place. The reflected light will interfere with the incident light, and in the far field this leads to maxima and minima in the radiated power per unit solid angle. The structure of the

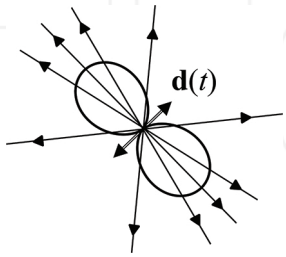

Figure 1. The electric dipole moment $\mathbf{d}(t)$ oscillates along the direction indicated by the double-headed arrow. The field lines of the Poynting vector come out of the dipole, and run radially outward. The solid curve is a polar diagram of the power per unit solid angle. No radiation is emitted along the dipole axis, and the maximum intensity is emitted perpendicular to the dipole axis.

http://dx.doi.org/10.5772/66459

angular power distribution of the transmitted light in the far field depends on the value of the critical angle and the distance between the particle and the surface. Usually, when a traveling plane wave is incident upon an interface, the transmitted wave is again traveling, and is bent toward the normal. When the angle of incidence approaches 90°, the transmitted wave is still traveling, and the angle of transmission is called the critical angle (for transmission). In the dipole spectrum, evanescent waves are present, and they are still transmitted as traveling waves, provided the wavelength is not too small. Therefore, above the critical transmission angle, all transmitted light comes from evanescent dipole waves, and this can lead to a large lobe in the power distribution above the critical angle [4]. Rather than considering the effects in the far field, we shall here present results for the power flow in the near field. We shall illustrate that interference gives rise to interesting flow patterns, including singularities, vortices, and strings of vortices. We also show that transmission in the near field exhibits interesting features.

2. Dipole radiation in free space

The oscillating dipole moment can be written as

$$\mathbf{d}(t) = d_{\mathrm{o}}\hat{\mathbf{u}}\cos(\omega t), \tag{1}$$

where d_{o} is the amplitude of the oscillation, and $\hat{\mathbf{u}}$ is a unit vector representing the direction of oscillation. Let $\mathbf{r}$ be the position vector of a field point, with respect to the location of the dipole, and let r be the length of $\mathbf{r}$. Then, $\hat{\mathbf{r}} = \mathbf{r}/r$ is the unit vector into the direction of the field point. The dimensionless distance between the dipole and the field point is defined as $q = k_{\mathrm{o}}r$, with $k_{\mathrm{o}} = \omega/c$ the wave number of the light. On this scale, a distance of 2π corresponds to one wave length. The emitted electric field has the form

$$\mathbf{E}(\mathbf{r}, t) = \mathrm{Re}[\mathbf{E}(\mathbf{r})e^{-i\omega t}], \tag{2}$$

with $\mathbf{E}(\mathbf{r})$ the complex amplitude, and a similar expression holds for the magnetic field $\mathbf{B}(\mathbf{r}, t)$. We define the constant

$$\zeta = \frac{k_{\mathrm{o}}^3 d_{\mathrm{o}}}{4\pi\varepsilon_{\mathrm{o}}}. \tag{3}$$

The dimensionless complex amplitudes $\mathbf{e}(\mathbf{r})$ and $\mathbf{b}(\mathbf{r})$ of the fields are introduced as

$$\mathbf{E}(\mathbf{r}) = \zeta\,\mathbf{e}(\mathbf{r}), \tag{4}$$

$$\mathbf{B}(\mathbf{r}) = \frac{\zeta}{c}\mathbf{b}(\mathbf{r}). \tag{5}$$

We then obtain for an electric dipole [5]

$$\mathbf{e}(\mathbf{r}) = \left\{ \hat{\mathbf{u}} - (\hat{\mathbf{r}} \cdot \hat{\mathbf{u}})\hat{\mathbf{r}} + [\hat{\mathbf{u}} - 3(\hat{\mathbf{r}} \cdot \hat{\mathbf{u}})\hat{\mathbf{r}}] \frac{i}{q} \left(1 + \frac{i}{q} \right) \right\} \frac{e^{iq}}{q}, \tag{6}$$

$$\mathbf{b}(\mathbf{r}) = (\hat{\mathbf{r}} \times \hat{\mathbf{u}}) \left(1 + \frac{i}{q} \right) \frac{e^{iq}}{q}. \tag{7}$$

The time-averaged Poynting vector for radiation in free space is given by

$$\mathbf{S}(\mathbf{r}) = \frac{1}{2\mu_o} \mathrm{Re}[\mathbf{E}(\mathbf{r}) \times \mathbf{B}(\mathbf{r})^*]. \tag{8}$$

For an electric dipole, we split off a factor:

$$\mathbf{S}(\mathbf{r}) = \frac{\zeta^2}{2\mu_o c} \boldsymbol{\sigma}(\mathbf{r}), \tag{9}$$

so that

$$\boldsymbol{\sigma}(\mathbf{r}) = \mathrm{Re}[\mathbf{e}(\mathbf{r}) \times \mathbf{b}(\mathbf{r})^*], \tag{10}$$

With the above expressions for $\mathbf{e}(\mathbf{r})$ and $\mathbf{b}(\mathbf{r})$, we find

$$\boldsymbol{\sigma}(\mathbf{r}) = \frac{1}{q^2} \hat{\mathbf{r}} \sin^2 \alpha, \tag{11}$$

and here α is the angle between the dipole axis (e.g., the direction of vector $\hat{\mathbf{u}}$) and the observation direction $\hat{\mathbf{r}}$. Since the vector $\boldsymbol{\sigma}(\mathbf{r})$ is proportional to $\hat{\mathbf{r}}$, the field lines of the vector field are straight, and run radially outward from the site of the dipole. This is shown in **Figure 1**. No power is emitted along the dipole axis ($\alpha = 0$), and the power per unit solid angle is maximum in the direction perpendicular to the dipole axis ($\alpha = \pi/2$).

3. Dipole radiation near a mirror

The simplest interface is a flat, infinite, and perfect mirror. We take the surface of the mirror as the xy-plane, and the dipole is located on the positive z-axis, at a distance H above the mirror. The dipole direction vector $\hat{\mathbf{u}}$ makes an angle γ with the positive z-axis, and we take $\hat{\mathbf{u}}$ in the yz-plane. Therefore,

$$\hat{\mathbf{u}} = \mathbf{e}_y \sin\gamma + \mathbf{e}_z \cos\gamma. \tag{12}$$

The electric field above the mirror is equal to the field of the dipole plus the electric field of an image dipole located at a distance H below the mirror on the z-axis, as illustrated in **Figure 2**, and the same holds for the magnetic field. The dipole moment direction of the image dipole is

http://dx.doi.org/10.5772/66459

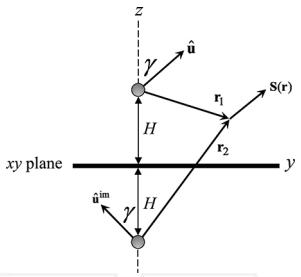

Figure 2. The electric dipole is located at a distance H above a flat mirror (xy-plane), and the image dipole is located at a distance H below the surface. Vectors $\mathbf{r}_1$ and $\mathbf{r}_2$ are the position vectors of the field point with respect to the location of the dipole and the image dipole, respectively. The field point is represented by the position vector $\mathbf{r}$ with respect to the origin of coordinates. This vector is not shown here.

$$\hat{\mathbf{u}}^{\text{im}} = -\ \mathbf{e}_y \sin\gamma + \mathbf{e}_z \cos\gamma. \tag{13}$$

The complex amplitudes of the electric and magnetic fields of the dipole are given by Eqs. (6) and (7), but with $\mathbf{r}$ replaced by the position vector of the field point relative to the dipole location. We indicate this vector by $\mathbf{r}_1$. Let $\mathbf{r}$ be the position vector of the field point where we wish to evaluate the fields. We see from **Figure 2** that

$$\mathbf{r}_1 = \mathbf{r} - H\mathbf{e}_z. \tag{14}$$

The coordinates of the field point only come in through $\hat{\mathbf{r}}$ and q in Eqs. (6) and (7), so we replace $\hat{\mathbf{r}}$ by $\hat{\mathbf{r}}_1$, and q by $q_1 = k_o r_1$. Similarly, the fields of the image dipole are found by replacing $\mathbf{r}$ by

$$\mathbf{r}_2 = \mathbf{r} + H\mathbf{e}_z, \tag{15}$$

q by $q_2 = k_o r_2$, and $\hat{\mathbf{u}}$ by $\hat{\mathbf{u}}^{\text{im}}$. With the fields $\mathbf{e}(\mathbf{r})$ and $\mathbf{b}(\mathbf{r})$ constructed, the Poynting vector follows from Eq. (10). It is easy to verify that for $z = 0$, e.g., just above the mirror surface, the Poynting vector is along the surface.

4. Computation of field lines

With the above method, the Poynting vector $\boldsymbol{\sigma}(\mathbf{r})$ can be computed for a given field point $\mathbf{r}$. We shall use dimensionless Cartesian coordinates $\overline{x} = k_o x$, $\overline{y} = k_o y$ and $\overline{z} = k_o z$, and the dimensionless distance $h = k_o H$. The Poynting vector is a function of $\overline{x}$, $\overline{y}$ and $\overline{z}$. Therefore, it is better to write $\boldsymbol{\sigma}(\mathbf{q})$ instead of $\boldsymbol{\sigma}(\mathbf{r})$, with $\mathbf{q} = k_o \mathbf{r}$. We shall do so from now on. The only free parameters are h and γ. A field line of the vector field $\boldsymbol{\sigma}(\mathbf{q})$ is a curve such that for each point $\mathbf{q}$ on the curve the vector $\boldsymbol{\sigma}(\mathbf{q})$ is on the tangent line. Let $\mathbf{q}(t)$ be a parameter representation of a field line, with t an arbitrary dummy variable. Then $\mathbf{q}(t)$ must be a solution of

$$\frac{\mathrm{d}}{\mathrm{d}t}\mathbf{q}(t) = \boldsymbol{\sigma}(\mathbf{q}(t)). \tag{16}$$

In Cartesian coordinates this becomes:

$$\frac{\mathrm{d}}{\mathrm{d}t}\overline{x}(t) = \boldsymbol{\sigma}_x(\overline{x}(t), \overline{y}(t), \overline{z}(t)), \tag{17}$$

and similarly for $\overline{y}(t)$ and $\overline{z}(t)$, so this is a set of three differential equations. The independent variable t does not appear explicitly, and such equations are called autonomous. The solution is determined by an initial point $(\overline{x}_\mathrm{o}, \overline{y}_\mathrm{o}, \overline{z}_\mathrm{o})$.. The field line through this point is found by solving Eq. (16). We set $t = 0$ at the initial point. The direction of the field line is the direction along the curve that follows from increasing t. So, the field line runs from the initial point into the direction that corresponds to the solution with $t > 0$. The solution with $t < 0$ is the part of the field line that runs toward the initial point.

Obviously, the differential Eq. (16) will in general need to be solved numerically. An interesting exception is the case for an arbitrary (elliptical) dipole in free space for which an analytical solution can be obtained, as reported in Ref. [6]. We use *Mathematica* to solve the set and produce the field line pictures. For two-dimensional problems, the routine StreamPlot only requires the expression for $\boldsymbol{\sigma}$ as a function of $\overline{x}$, $\overline{y}$ and $\overline{z}$. The initial points $(\overline{x}_\mathrm{o}, \overline{y}_\mathrm{o}, \overline{z}_\mathrm{o})$ are called StreamPoints and can be specified. Alternatively, one can let *Mathematica* select these initial points. This is much faster, and works well to get an initial picture. However, in this approach *Mathematica* cuts off field lines when they get too close together, and that does not necessarily look too good.

Finally, field lines are determined by the direction of vector $\boldsymbol{\sigma}$ at a point $\mathbf{q}$, and not by its direction. Therefore, the vector fields $\boldsymbol{\sigma}(\mathbf{q})$ and $f(\mathbf{q})\boldsymbol{\sigma}(\mathbf{q})$, with $f(\mathbf{q})$ an arbitrary positive function of $\mathbf{q}$, have the same field lines. This can also be seen by making the change of variables $t = f(\mathbf{q})t'$. We then get

$$\frac{\mathrm{d}}{\mathrm{d}t}\mathbf{q}(t) = f(\mathbf{q}(t))\sigma(\mathbf{q}(t)), \tag{18}$$

and this equation has the same solutions for the field lines as Eq. (16). It just gives a different parametrization of the curves. A popular choice is $f(\mathbf{q}) = 1/|\boldsymbol{\sigma}(\mathbf{q})|$, which makes the right-hand side of Eq. (18) a unit vector. For the mirror problem, the fields diverge in the neighborhood of the dipole, and a good choice seems to be $f(\mathbf{q}) = q_1^5$.

5. Field lines in the symmetry plane

The dipole direction vector $\hat{\mathbf{u}}$ and the direction of its image $\hat{\mathbf{u}}^{\mathrm{im}}$ are both in the yz-plane. If we take a field point in the yz-plane, then also $\hat{\mathbf{r}}$ is in the yz-plane, and therefore, $\mathbf{e}(\mathbf{r})$ from Eq. (6) is in the yz-plane, and the same holds for the complex amplitude of the image electric field. From

http://dx.doi.org/10.5772/66459

Eq. (7), we see that the complex amplitudes of the magnetic dipole field and the magnetic image field are along the x-axis if the field point is in the yz-plane. Therefore, the Poynting vector from Eq. (10) is in the yz-plane if the field point is in the yz-plane. Consequently, any field line through a point in the yz-plane stays in the yz-plane. This plane is the symmetry plane for the dipole near the mirror. For field lines off the symmetry plane the field lines will be 3D curves, and the flow pattern is reflection symmetric in the yz-plane. Field lines in 3D are difficult to visualize, so we shall only consider field lines in the symmetry plane.

Figure 3 shows the flow lines of energy for a dipole oscillating along the z-axis ($\gamma = 0$). The field line pattern is rotation symmetric around the z-axis. The field lines that run toward the surface smoothly bend away from the surface upon approach. At the origin of coordinates we have a singularity, since the field lines that come out of the dipole and run straight down split there. This point is marked with a white circle. **Figure 4** shows the flow pattern for a dipole oscillating parallel to the surface ($\gamma = \pi/2$). The pattern is reflection symmetric in the z-axis, so only the region $\overline{y} < 0$ is shown. Just left of the dipole are two singularities. It seems that a field

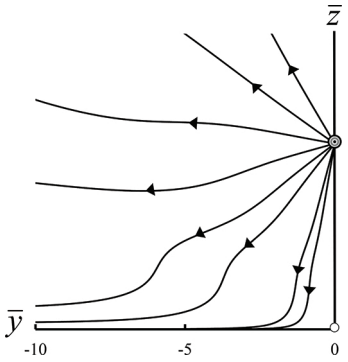

Figure 3. The dipole is located at a distance $h = 2\pi$ above the mirror, and the dipole oscillates along the z-axis.

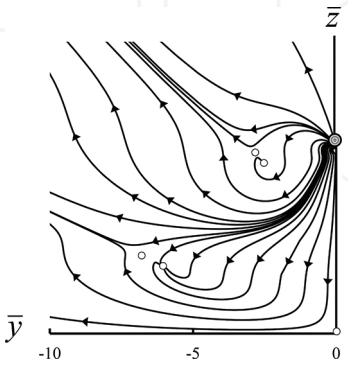

Figure 4. The dipole is located at a distance $h = 2\pi$ above the mirror, and the dipole oscillates parallel to the xy-plane.

line ends at the lower singularity, but this is essentially a minuscule vortex. The higher of the two is a singularity where field lines "collide." There is again a singularity right below the dipole on the mirror surface, and two other singularities appear at greater distances.

Figure 5 shows the field lines for a dipole oscillating under 45° with the z-axis ($\gamma = \pi/4$). Numerous singularities and vortices appear for this case. Vortex c is close to the dipole, and is similar to the small vortex in **Figure 4**. Vortices a and b have a greater extent, although they are still of subwavelength dimension. Some field lines come out of the dipole and swirl around vortex a, and some pass by vortex b. Interestingly, there are field lines that emanate from vortex a and end up at the center of vortex b. This seems to represent energy flowing from vortex a to vortex b, but that is not the case. Only the dipole is a source for the vector field of the Poynting vector. The singularity at the point labeled S seems like a bump in the road for the field lines that pass nearby. It can be shown analytically [7] that this singularity is a point on a singular circle in the plane of the mirror. The circle goes through the origin of coordinates and singularity S, and singularity S is located at $\overline{y} = -h \tan\gamma$. For $\gamma = \pi/4$ this is at $\overline{y} = -h$, and for the case of **Figure 5** this is at $\overline{y} = -h = -2\pi$. To the right of the z-axis, not shown in **Figure 5**, there seems to be no interesting structure.

When the dimensionless distance h between the dipole and the surface increases, so does the number of vortices. In **Figures 3–5**, this distance was taken as $h = 2\pi$, corresponding to one wavelength. In **Figure 6**, this distance is $h = 8\pi$, and angle γ is the same as in **Figure 5**. We notice

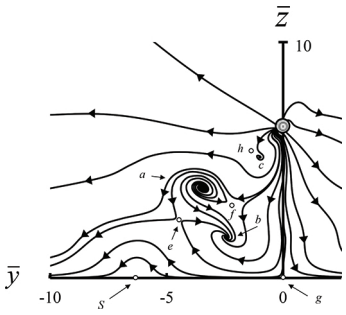

Figure 5. The dipole is located at a distance $h = 2\pi$ above the mirror, and the dipole oscillates under 45° with the z-axis.

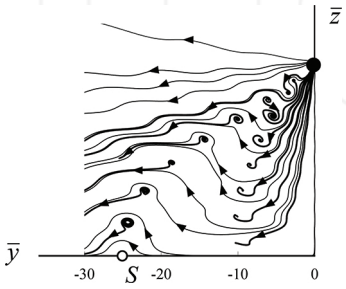

Figure 6. The dipole is located at a distance $h = 8\pi$ above the mirror, and the dipole oscillates under 45° with the z-axis.

http://dx.doi.org/10.5772/66459

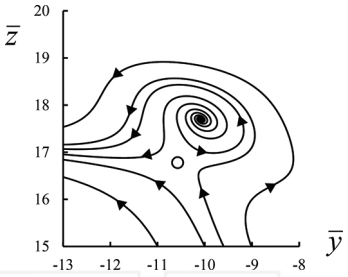

Figure 7. Enlargement of a vortex of **Figure 6**.

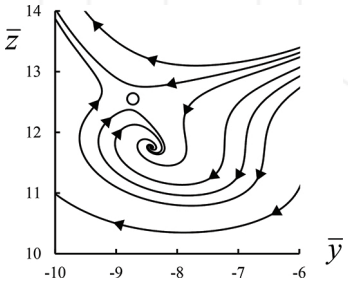

Figure 8. Enlargement of a vortex of **Figure 6**.

numerous vortices in the flow line pattern. The field lines rotate counterclockwise around the singularities that are close to the *z*-axis. **Figure 7** shows an enlargement of one of these vortices, and it follows from the pattern that there must be another singularity nearby. The vortices on the left have a clockwise rotation and **Figure 8** shows an enlargement. For the vortices on the left the field lines come out of the center of the vortex, and for the vortices on the right the field lines end at the center of the vortex, as in **Figures 7** and **8**, respectively. In **Figure 6**, the field lines that start or end at a vortex are drawn in bold. Many other field lines are present. They run from the dipole to infinity, either without coming in the neighborhood of the vortices (the four field lines on top of the picture) or they cross the array of vortices once or twice.

6. Location of the vortices

At a singularity, the Poynting vector vanishes. This can be due to $\mathbf{E}(\mathbf{r}) = 0$ or $\mathbf{B}(\mathbf{r}) = 0$ or $\mathbf{E}(\mathbf{r}) \times \mathbf{B}(\mathbf{r})^*$ is imaginary. We have found that for singularities that appear when field lines split or collide, $\mathbf{E}(\mathbf{r}) \times \mathbf{B}(\mathbf{r})^*$ is imaginary. Singularities at the center of a vortex are due to the vanishing of the magnetic field. For field lines in the *xy*-plane, the complex amplitude of the magnetic field is along the *x*-axis. For $\mathbf{B}(\mathbf{r})_x$ to be zero, both the real and imaginary part have to be zero at the same point. With the expressions for the magnetic field of source and image, we find that $\mathrm{Re}[\mathbf{B}(\mathbf{r})_x] = 0$ leads to

$$\frac{q_1\cos q_1-\sin q_1}{q_1^3}\left[\overline{y}\cos\gamma+(h-\overline{z})\sin\gamma\right]+\frac{q_2\cos q_2-\sin q_2}{q_2^3}\left[\overline{y}\cos\gamma+(h+\overline{z})\sin\gamma\right]=0, \tag{19}$$

and similarly $\mathrm{Im}[\mathbf{B}(\mathbf{r})_x]=0$ gives

$$\frac{q_1\sin q_1+\cos q_1}{q_1^3}\left[\overline{y}\cos\gamma+(h-\overline{z})\sin\gamma\right]+\frac{q_2\sin q_2+\cos q_2}{q_2^3}\left[\overline{y}\cos\gamma+(h+\overline{z})\sin\gamma\right]=0. \tag{20}$$

The solutions of Eq. (19) are curves in the yz-plane, and Eq. (20) also represents a set of curves in the yz-plane. At intersections between these sets of curves the magnetic field is zero, and this corresponds to the center of a vortex. **Figure 9** shows the curves for the same parameters as

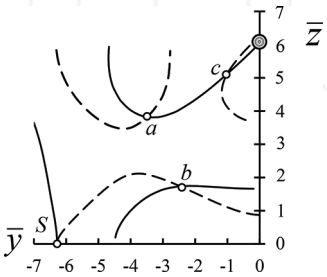

Figure 9. The vortices of **Figure 5** appear at intersections between the solid and dashed curves.

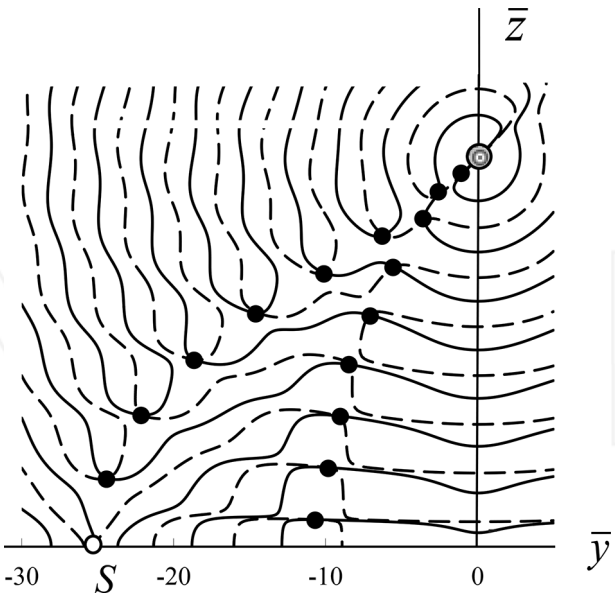

Figure 10. The vortices of **Figure 6** appear at intersections between the solid and dashed curves, and these intersections are indicated by black dots.

http://dx.doi.org/10.5772/66459

shown in **Figure 5**. The solid lines are the solutions of Eq. (19) and the dashed lines are the solutions of Eq. (20). The three intersections *a*, *b*, and *c* are the centers of the three vortices in **Figure 5**. Interestingly, at the center of the bump on the mirror, labeled *S*, the magnetic field also vanishes. This point is located at

$$\overline{y} = -h \tan\gamma, \quad \overline{z} = 0, \tag{21}$$

and it is easy to check that this is indeed a solution of both Eqs. (19) and (20). Here, the magnetic field is zero, but there is no vortex. For the case of the parameters for **Figure 6**, the solutions of Eqs. (19) and (20) are shown in Figure 10.

7. Vortex strings

In **Figure 10**, the intersections between the solid and dashed curves are not always precisely to determine and this gets worse with increasing *h*. By manipulating Eqs. (19) and (20), a different set of equations can be obtained. We find [8]

$$\begin{aligned}[(q_1q_2+1)\cos(q_2{-}q_1)+(q_2{-}q_1)\sin(q_2{-}q_1)][\overline{y}\cos\gamma+(h+\overline{z})\sin\gamma]\\ +\left(\frac{q_2}{q_1}\right)^3(q_1^2+1)[\overline{y}\cos\gamma+(h{-}\overline{z})\sin\gamma]=0,\end{aligned} \tag{22}$$

$$(q_1q_2+1)\sin(q_2{-}q_1)=(q_2{-}q_1)\cos(q_2{-}q_1). \tag{23}$$

The solid curve in **Figure 11** is the solution of Eq. (22) and the dashed curves are the solutions of Eq. (23). Vortices appear at the intersections. The parameters are the same as for **Figure 10**. Interestingly, Eq. (23) is independent of the orientation angle γ of the dipole. When γ varies, the solid curve rotates with it, but the dashed curves stay the same. The solid curve starts at the location of the dipole and runs to point *S* on the mirror, as can easily be checked from Eq. (21).

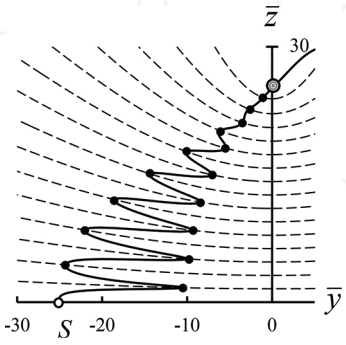

Figure 11. The black dots are the intersections between the solid curve and the dashed curves. These points correspond to the location of vortices, and here we have used the same parameters γ and *h* as for **Figure 10**.

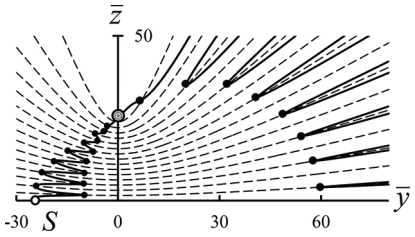

Figure 12. The figure shows a larger view of the picture in **Figure 11**.

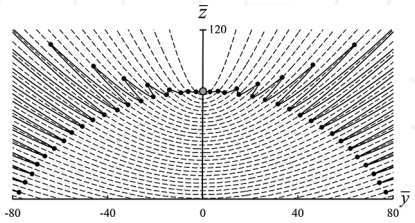

Figure 13. The figure shows vortex strings for $\gamma = \pi/2$ and $h = 30\pi$.

The vortices in **Figure 11** appear to lie on two 'strings'. The left string starts at the dipole and runs to point S on the mirror. The second string is in between the left string and the z-axis. It can be seen from **Figure 6** that all the vortices on the left string have a counterclockwise rotation, as in **Figure 7**. On the right string the vortices have a clockwise rotation, as in **Figure 8**. **Figure 12** shows a larger view of the same graph as in **Figure 11**. The solid line passes the dipole and continues in the upper right part of the graph. It appears that far away there are also intersections between the solid curve and the dashed curves, and these correspond also to the location of vortices. The vortices appear to lie on a third string. It can be shown that these vortices have a counterclockwise rotation.

The left string ends at point S on the mirror. The location of this point depends on the dipole angle γ, according to Eq. (21). When γ increases, the point moves to the left, and for $\gamma \to \pi/2$ the point moves to infinity. **Figure 13** shows the string pattern for $\gamma = \pi/2$ and $h = 30\pi$. The field line pattern must be reflection symmetric in the z-axis, and so is the string pattern. We see that a fourth string of vortices appears, and from symmetry it follows that these have a clockwise rotation. When we look again at **Figure 12**, the solid curve must intersect the dashed curves outside the picture in the upper right corner. Therefore, there is a fourth string very far away, and outside the picture. Apparently, there are always four vortex strings in electric dipole radiation near a mirror.

8. Dielectric interface

An interesting generalization of the free dipole near the mirror is the case of a dipole embedded in a dielectric medium, and near an interface with another dielectric material. For this

http://dx.doi.org/10.5772/66459

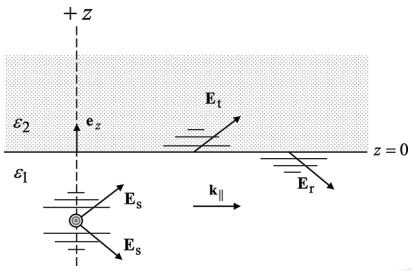

Figure 14. The figure shows the setup for a dipole embedded in a dielectric material and near an interface with another dielectric material.

problem, we reverse the z-axis, as compared to **Figure 2**, and we place the dipole on the negative z-axis, at a distance H below the interface. This is illustrated in **Figure 14**. The dielectric constant of the embedding medium is ε_1 and the substrate has dielectric constant ε_2. The corresponding indices of refraction are $n_1 = \sqrt{\varepsilon_1}$ and $n_2 = \sqrt{\varepsilon_2}$, respectively. The analysis of this system is considerably more complicated than the mirror problem. For simplicity of notation, we shall assume that the dipole oscillates along the z-axis, e.g., $\hat{\mathbf{u}} = \mathbf{e}_z$. The approach here is to represent the source fields (6) and (7) by an angular spectrum of plane waves. The reflection and transmission of each partial wave is accounted for by the appropriate Fresnel coefficients. A partial wave can be traveling or evanescent, and in **Figure 14** this is schematically indicated by vectors and dashed parallel lines, respectively. In each triad of partial source, reflected and transmitted waves the parallel component of each of the three wave vectors is the same. Upon reflection and transmission only the z-component of a wave vector can change. Set $\alpha = k_{||}/k_o$, which is the dimensionless magnitude of the parallel component of each wave vector. The dimensionless z-components of the wave vectors can be expressed in terms of the functions

$$v_i = \sqrt{n_i^2 - \alpha^2}\,, \quad i = 1, 2. \tag{24}$$

The wave vector of an incident partial wave of the source field has a z-component of $k_o v_1$. Similarly, the reflected and transmitted waves have wave vectors with z-components $-k_o v_1$ and $k_o v_2$, respectively. For $\alpha < n_i$, v_i is real, and the corresponding wave is traveling. For $\alpha > n_i$, v_i is positive imaginary, and the corresponding wave is evanescent. The Fresnel reflection and transmission coefficients for an incident p-polarized plane wave with parameter α are

$$R_p(\alpha) = \frac{\varepsilon_2 v_1 - \varepsilon_1 v_2}{\varepsilon_2 v_1 + \varepsilon_1 v_2}, \tag{25}$$

$$T_p(\alpha) = \frac{n_2}{n_1} \frac{2\varepsilon_1 v_1}{\varepsilon_2 v_1 + \varepsilon_1 v_2}. \tag{26}$$

For the dipole oscillating along the z-axis, all partial waves are p polarized.

The setup is rotation symmetric around the z-axis, so we only need to consider the solution in the yz-plane, with $y > 0$. Then the electric field is in the yz-plane, the magnetic field is along the

x-axis, and the Poynting vector is in the yz-plane. We obtain for the complex amplitudes of the dimensionless electric and magnetic reflected fields [9]

$$\mathbf{e}_{\mathrm{r}}(\mathbf{r}) = \frac{1}{\varepsilon_1}\int_0^\infty \mathrm{d}\alpha\, \alpha^2 R_p(\alpha)\left[\mathbf{e}_z \frac{i\alpha}{v_1} J_0(\alpha\overline{y}) - \mathbf{e}_y J_1(\alpha\overline{y})\right] e^{iv_1(h-\overline{z})}, \tag{27}$$

$$\mathbf{b}_{\mathrm{r}}(\mathbf{r}) = -\,\mathbf{e}_x \int_0^\infty \mathrm{d}\alpha \frac{\alpha^2}{v_1} R_p(\alpha) J_1(\alpha\overline{y}) e^{iv_1(h-\overline{z})}, \tag{28}$$

and for the transmitted fields we find

$$\mathbf{e}_{\mathrm{t}}(\mathbf{r}) = \frac{1}{n_1 n_2}\int_0^\infty \mathrm{d}\alpha \frac{\alpha^2}{v_1} T_p(\alpha)[\mathbf{e}_z i\alpha J_0(\alpha\overline{y}) + \mathbf{e}_y v_2 J_1(\alpha\overline{y})] e^{i(v_1 h + v_2\overline{z})}, \tag{29}$$

$$\mathbf{b}_{\mathrm{t}}(\mathbf{r}) = -\,\mathbf{e}_x \frac{n_2}{n_1}\int_0^\infty \mathrm{d}\alpha \frac{\alpha^2}{v_1} T_p(\alpha) J_1(\alpha\overline{y}) e^{i(v_1 h + v_2\overline{z})}. \tag{30}$$

Here, J_0 and J_1 are Bessel functions. These four fields are integral representations of the solutions, and, obviously, these integrals need to be computed numerically. On the z-axis we have $\overline{y} = 0$, and since $J_1(0) = 0$ we see that the magnetic fields vanish on the z-axis. The magnetic source field, Eq. (7), also vanishes on the z-axis. Therefore, the Poynting vector is zero on the z-axis, and so the z-axis is a singular line of the flow lines pattern.

For the case of **Figure 15**, we have $n_1 = 1$ and $n_2 = 2$. The energy flows from a thinner to a thicker medium. Upon transmission, the field lines of the Poynting vector bend toward the normal, just like optical rays would do for this case. However, the angle of incidence and the angle of transmission for the Poynting vector are not related by Snell's law, as the

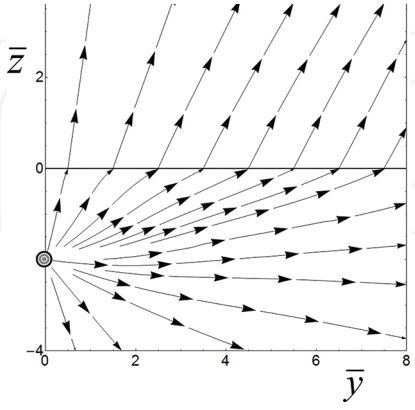

Figure 15. The figure shows the transmission through an interface into a thicker medium.

http://dx.doi.org/10.5772/66459

corresponding angles for optical rays are. The critical angle for this interface is 30°, and we see that away from the z-axis the field lines leave the interface under approximately 30°. This critical angle corresponds to an angle of incidence of 90°, and we see from the figure that the field lines do not approach the interface under 90°. The reason that the field lines leave the interface under approximately the critical angle is that the Fresnel transmission coefficient has a sharp maximum at this angle. The angular spectrum is a superposition of waves with all angles of incidence, and extends into the evanescent region as well. The transmission coefficient favors partial waves that approach the interface under about 90°. These are the partial waves that are on the borderline of the traveling and the evanescent regions of the angular spectrum.

More interesting is the case for transmission into a thinner medium, as illustrated in **Figure 16**. The indices of refraction are $n_1 = 2$ and $n_2 = 1$. On crossing the interface, the field lines bend away from the normal, just like optical rays. We see here that the field lines are more curved than in **Figure 15**. Some of the field lines that entered the n_2 medium bend down, and then cross the interface again. The field lines run through the n_1 material for a short distance and then bend up and cross the interface again into the n_2 region. This oscillation of energy back and forth through the interface persists over long distances. **Figure 17** shows an enlargement of the first dip of the field lines below the interface. We see that a vortex appears in medium n_2,

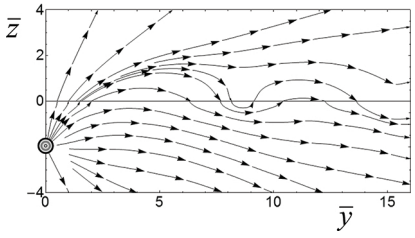

Figure 16. The figure shows the transmission through an interface to a thinner medium.

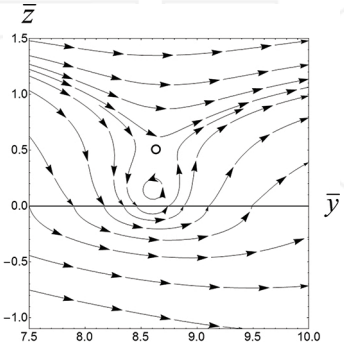

Figure 17. Enlargement of a part of **Figure 16**. Just above the first dip of the field lines under the interface a vortex appears. Above the vortex is a singularity, indicated by a white circle.

just above the dip of the field lines under the interface. And just above the vortex, we necessarily have a singularity because near this point the field lines run in opposite directions.

9. Dipole in between mirrors

An interesting variation of the mirror problem is the case for a dipole in between parallel mirrors, as depicted in **Figure 18**. A second mirror is placed at a distance D above the first mirror. Now, the dipole has a mirror image in both mirrors. In order to satisfy the boundary conditions at both mirrors, a mirror image must have again an image in the other mirror, and so on. This leads to an infinite sequence of images. Let us label the images with m. We then find that the images are located at

$$z_m = (m + \frac{1}{2})D + (-1)^m(H - \frac{1}{2}D), \tag{31}$$

with m integer. For $m = 0$, this is the actual dipole in **Figure 18**. The image with $m = -1$ is the image dipole from **Figure 2**. Images with m even have a dipole orientation vector $\hat{\mathbf{u}}$ and images with m odd have $\hat{\mathbf{u}}^{\text{im}}$ as orientation vector.

This can be combined as

$$\hat{\mathbf{u}}_m = (-1)^m \mathbf{e}_y \sin\gamma + \mathbf{e}_z \cos\gamma, \tag{32}$$

for the orientation of image m. The dimensionless distance between the mirrors is denoted by $\delta = k_o D$.

Figure 19 shows the energy flow pattern for a horizontal dipole midway between the mirrors. The distance between the mirrors is $\delta = 4\pi$. Most of the radiation is emitted in the vertical direction. It travels to the mirrors, and there the field lines bend and continue horizontally. No radiation is emitted along the dipole axis, and we see that the line $\bar{z} = 2\pi$ is a singular line. Field lines approach this line from above and below, and then stop at this line. Consequently, the Poynting vector has to be zero on this line. For **Figure 20**, we have $\gamma = \pi/4$ and $\delta = \pi$, and the dipole is midway between the mirrors. We notice the appearance of two vortices very close to the dipole (subwavelength distance), and the rotation is counterclockwise for both. Some of

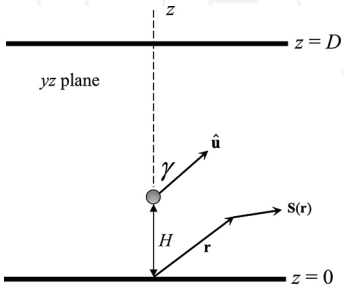

Figure 18. The figure shows the setup for the dipole in between mirrors.

http://dx.doi.org/10.5772/66459

the field lines run downward to the right swing up turn around (outside the figure) and end up running to the left. Similarly, some field lines start toward top-left, and then turn around, swing by the dipole, and then run off to the right. In **Figure 21**, we have again a horizontal

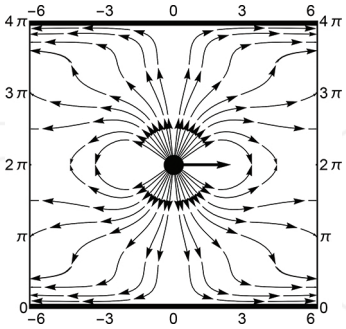

Figure 19. The figure shows the flow lines of energy for a horizontal dipole midway between the mirrors.

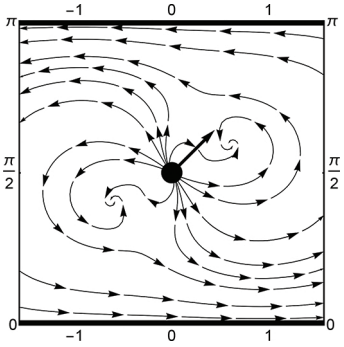

Figure 20. The figure shows the flow lines of energy for a dipole midway between the mirrors, and oscillating under 45° with the *z*-axis.

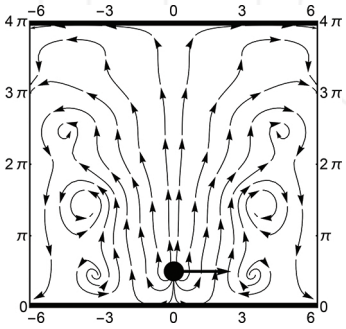

Figure 21. The figure shows the flow lines of energy for a dipole close to the lower mirror and oscillating horizontally.

dipole, but it is now closer to the mirror on the bottom. Numerous vortices appear in the flow pattern.

10. Conclusions

An oscillating electric dipole in free space emits its energy along straight lines. Most radiation is emitted perpendicular to the dipole axis, and none comes out along the dipole axis. We have studied the effect of a nearby interface on this flow pattern. Reflection of radiation at the interface leads to interference between the directly emitted radiation and the reflected radiation. A mirror is impenetrable for radiation, and so all radiation bounces back at the interface. This also implies that the field lines of energy flow must be parallel to the mirror at the mirror surface. This effect is shown in **Figure 3** for a dipole oscillating perpendicular to the surface, and one wavelength away from the surface. The radiation comes out of the dipole, more or less as for emission in free space, but at the mirror surface the field lines bend, and the energy flows away along the mirror surface. For a dipole oscillating parallel to the surface, a typical flow pattern is shown in **Figure 4**. Again, at the mirror surface the field lines run away parallel to the surface, but in between the surface and the dipole several singularities appear, and there is also a vortex very close to the dipole. For the case shown in **Figure 5**, the dipole oscillates under 45° with the normal to the surface, and we see that two large vortices appear and one very small one. The rotation direction of the energy flow in the two large vortices is in opposite directions, and some energy flows from one vortex to the other. When the distance between the dipole and the surface is much larger than a wavelength, numerous tiny (subwavelength) vortices appear, and we found that the vortices are located on a set of four strings. This is shown most clearly in **Figure 13**.

When the surface is an interface between two dielectrics, we also need to consider the radiation transmitted into the substrate. Here, we only consider the simplest case of a dipole oscillating perpendicular to the interface. This can be generalized to arbitrary oscillation directions, and also to the case where the surface is an interface with a layer of material, and this layer is located on a substrate of yet another kind of material [10]. **Figure 15** illustrates a typical case of transmission into a thicker medium. The field lines bend toward the normal, just like optical rays would. However, the refraction angle for the flow lines does not follow Snell's law for optical rays. **Figure 16** shows field lines for transmission into a thinner medium. Now the field lines bend away from the normal, but some field lines bend so much that they return to the other side of the interface. There is oscillation of energy back and forth through the interface. An enlargement is shown in **Figure 17**, and we observe that a vortex appears just above the location where the energy goes back and forth through the interface.

We have also considered the case where the oscillating dipole is located in between two mirrors. For a horizontal dipole, the emitted radiation bends near the surfaces of the two mirrors, and then flows away horizontally, as shown in **Figure 19**. For the case in **Figure 20**, the dipole oscillates under 45° with the normal. Two vortices appear. Some of the radiation that is emitted to the bottom-right of the picture originally flows to the right along the surface of the lower mirror, but then turns around, swings by the dipole, and then continues to the left, along

http://dx.doi.org/10.5772/66459

the surface of the top mirror. When the dipole is not located midway between the mirrors, as in **Figure 21**, numerous vortices appear, and the pattern repeats indefinitely to the left and right in the range outside the picture.

Author details

Xin Li[1], Henk F. Arnoldus[2]* and Zhangjin Xu[2]

*Address all correspondence to: hfa1@msstate.edu

1 Department of Physics, Millersville University, Millersville, PA, USA

2 Department of Physics and Astronomy, Mississippi State University, Mississippi State, MS, USA

References

[1] Born M, Wolf E. Principles of Optics. 6th ed. Pergamon: Oxford; 1980. Ch. 3.

[2] Griffiths D J. Introduction to Electrodynamics. 2nd ed. Upper Saddle River: Prentice Hall; 1989. p. 323.

[3] Li X, Pierce D M, Arnoldus H F. Redistribution of energy flow in a material due to damping. Opt. Lett. 2011; **36**: 349–351.

[4] Arnoldus H F, Foley J T. Transmission of dipole radiation through interfaces and the phenomenon of anti-critical angles. J. Opt. Soc. A. 2004; **21**: 1109–1117.

[5] Jackson J D. Classical Electrodynamics. 3rd ed. New York: Wiley; 1999. p. 411.

[6] Shu J, Li X, Arnoldus H F. Energy flow lines for the radiation emitted by a dipole. J. Mod. Opt. 2008; **55**: 2457–2471.

[7] Li X, Arnoldus H F. Electric dipole radiation near a mirror. Phys. Rev. A. 2010; **81**(053844): 1–10.

[8] Li X, Arnoldus H F. Vortex string in electric dipole radiation near a mirror. Opt. Commun. 2013; **305**: 76–81.

[9] Arnoldus H F, Berg M J, Li X. Transmission of electric dipole radiation through an interface. Phys. Lett. A. 2014; **378**: 755–759.

[10] Arnoldus H F, Berg M J. Energy transport in the near field of an electric dipole near a layer of material. J. Mod. Opt. 2015; **62**: 244–254.